INVESTIGATION OF COHERENT SOURCES OF INFRARED RADIATION

under the direction of

A. L. Schawlow

Semi-Annual Status Report No. 3

for

NASA Research Grant NGR-05-020-166

National Aeronautics and Space Administration

Washington 25, D. C.

for the period

1 May to 31 October 1967

M. L. Report No. 1601

November 1967

Microwave Laboratory
W. W. Hansen Laboratories of Physics
Stanford University
Stanford, California

STAFF

NASA RESEARCH GRANT NGR-05-020-166

for the period

1 May – 31 October 1967

PRINCIPAL INVESTIGATOR

A. L. Schawlow, Professor

RESEARCH ASSISTANT

B. McCaul

INTRODUCTION

This program is concerned with new methods of generating and detecting far infrared radiation and with their applications to problems of physical interest. The over-all purpose is to advance the technology of the infrared region so that it may become as accessible for scientific investigations as the radio and optical portions of the spectrum.

PRESENT STATUS

Pulsed far-infrared lasers operate under conditions of electron density and discharge current such that at least two plasma effects may become evident. First, if the electron density is sufficiently high, the plasma is momentarily opaque to the lasering emission, thus permitting the population inversion to develop; the cavity, then, is Q-switched by the electron density. Second, if the laser pulse is emitted while a large electrical discharge current and its magnetic field exist and while the electron density is sufficiently high, plasma birefringence occurs. Plasma birefringence implies two apparent wavelengths inside the cavity for each frequency oscillation, and thus it implies a doubling of cavity modes. (Since two cavity wavelengths map to a single vacuum wavelength some confusion would arise if the cavity resonance spacing were used to deduce the spectral properties of the laser light.) Furthermore, the two waves are orthogonally polarized implying distinct polarization properties for the two cavity modes.

In this report we discuss the application of the Appleton-Hartree equations for the propagation of electromagnetic waves in a cold magneto-ionic medium without collisions, according to the plasma birefringence hypothesis. It is assumed that lasering begins during the moments of sharply-falling attenuation as the plasma frequency falls below the light frequency. The plasma birefringence is obtained for a simple model of the discharge current, magnetic field, and gain cross-section.

Comparisons with several published results are made, and the role of the implied electron density as a loss mechanism is discussed. Similar comments are made for the case of applied longitudinal magnetic fields on cw far-infrared lasers.

The contribution of the electron density to the index of refraction of a plasma is given by the Appleton-Hartree dispersion formulae[1] (neglecting collisions):

$$n^2 = 1 - \frac{X}{1 - \frac{1/2\ Y_T^2}{1-X} \pm \left[\frac{Y_T^4}{4(1-X)^2} + Y_L^2\right]^{1/2}} \qquad (1)$$

$$X = \left(\frac{\omega_p}{\omega}\right)^2 , \quad \omega_p^2 = \frac{Ne^2}{\epsilon_o m}$$

$$Y_L = \frac{\omega_c \cos\theta}{\omega} , \quad \omega_c = \frac{eB}{m}$$

$$Y_T = \frac{\omega_c \sin\theta}{\omega} ,$$

where θ equals the angle between wave normal and B, the magnetic field; N, e, and m refer to the electron density, charge, and mass. The light angular frequency is ω. The polarization of the two waves is given by

$$\rho = \frac{E_Y}{E_X} = \frac{i\ Y_T^2}{2\ Y_L(1-X)} \pm i\left\{\frac{Y_T^4}{4\ Y_L^2(1-X)^2} + 1\right\}^{1/2} \qquad (2)$$

For no magnetic field we have $n^2 = 1-X$. We assume that for a short time during the first instants of the pulsed discharge the atoms and molecular fragments of the original vapor are sufficiently ionized

that $X>1$ ($N > 9.8 \times 10^{15}$ per cm^3 for 337 μ, 3.9×10^{15} per cm^3 for 538 μ), the index of refraction is purely imaginary, and the medium reflects.[2] Lasering on the leading edge of the electron density pulse is unlikely; we consider the decreasing electron density on the trailing edge of the pulse. The center frequency of the cavity is thus being swept, in that the optical cavity length is being changed even though the physical length is not. The attenuation at the same time is steeply decreasing. The laser output frequency then is not only swept but is pulled by a time-varying cavity Q. The molecular linewidth in the HCN laser has been estimated to be about 8 MHz (using cw mode-pulling data and a mode-pulling model assuming a homogeneously-broadened line);[3] in far-infrared lasers the mode spacing, $c/2L$, where L is the cavity length, is large with respect to the molecular gain curve.

Magnetic field effects correspond to a finite but, in this application, very small value for Y; for the magnetic fields involved the light frequency is far above the electron cyclotron frequency. Two indices of refraction and two polarizations appear in the Appleton-Hartree formulas corresponding to upper and lower signs. We may relate indices of refraction and internal wavelengths with two kinds of mirror displacement data:

1. For oscillation at the same frequency, for instance at the center of the molecular gain curve, the two wavelengths are related through their common frequency:

$$\frac{c}{n_o \lambda_o} = \nu = \frac{c}{n_x \lambda_x} \quad ; \quad \frac{\lambda_x}{\lambda_o} = \frac{n_o}{n_x} \quad . \tag{3}$$

The subscripts o and x refer to ordinary and extraordinary waves; "extraordinary" implies magnetic field dependence, but in general both waves depend on the magnetic field.[1] The λ_o and λ_x are the two internal apparent average wavelengths corresponding to each external vacuum wavelength. In the cases considered here, we have $\lambda_x \geq \lambda_o$. These two infrared wavelengths can be inferred by measuring for each polarization the mirror displacement, $\lambda/2$, between adjacent mode numbers; from the wavelengths we infer the ratio of refractive indices for comparison with the theory.

2. The frequency of an ordinary-wave axial cavity mode is given by $(c/n_o L_o)(2L_o/\lambda_o)$ where $q = 2L_o/\lambda_o$ is the axial mode number. For oscillation at the same frequency, for instance at the center of the molecular gain curve, and for the same mode number, we have for two cavity lengths:

$$\frac{\lambda_x}{\lambda_o} = \frac{L_x}{L_o} = 1 + \frac{L_x - L_o}{L_o} = \frac{n_o}{n_x} \quad . \qquad (4)$$

Thus the two infrared wavelengths may also be inferred by measuring both the total cavity length and the mirror displacement between the two polarizations for the same mode number. For a large internal wavelength difference of a few parts in 10^4 the two polarizations are separated by several half-wavelengths of mirror displacement. In addition, transverse modes may be present. This method then is more useful for small internal wave differences where the mirror displacement between polarization modes is less than the linewidth.

Transverse Magnetic Field

Consider the transverse magnetic field of the discharge current itself in the situation of temporal overlap of the current and laser pulses. Neglecting longitudinal fields ($\theta = \pi/2$, $Y_L = 0$) we have from (1):

$$n_o^2 = 1-X$$

$$n_x^2 = 1 - \frac{X(1-X)}{1-X-Y_T^2}$$

$$\frac{\lambda_o}{\lambda_x} = \frac{n_x}{n_o} \cong 1 - \frac{XY_T^2}{2(1-X)^2} \quad , \quad \frac{XY_T^2}{2(1-X)^2} \ll 1 \quad . \qquad (5)$$

The polarization $\rho = 0$ for the ordinary wave and $\rho = \infty$ for the extraordinary wave. The E-vector of the ordinary wave is everywhere parallel to the local plasma current magnetic field, while the E-vector of the extraordinary wave is perpendicular. Thus the two laser modes must have their E-vector polarizations as seen in Fig. 1.

Values for Y_T^2 are estimated in the following way. Clearly the radial distribution of electron and current density, transverse magnetic field, and laser gain and mode volume is complex. We assume the current density is coincident spatially with the electron density and use a simple steady state model of the radial electron distribution;[4] the parameter of the Bessel function solution to the diffusion equation is adjusted so that the first zero appears at the tube wall, R ; then

$$N(r) = N(0)\, J_0 \left(\frac{2.4r}{R}\right) \quad .$$

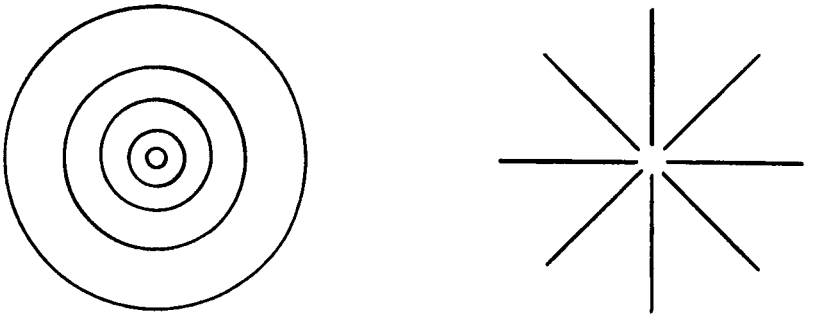

FIG. 1--(a) E-vector polarization direction for ordinary wave with respect to axis of maximum current. (b) E-vector polarization direction for extraordinary wave.

We substitute current density $j(r)$ for $N(r)$, apply Ampere's law for the transverse magnetic field, integrate over r, and find, in terms of an arbitrary radius r_o and the total peak current I,

$$B_\theta(r_o) = \frac{\mu_o I}{2\pi R} \frac{J_1\left(\frac{2.4 r_o}{R}\right)}{J_1(2.4)} .$$

Figure 2 is a schematic of the radial distribution of the current density and magnetic induction. Note B_θ has a maximum away from the wall and it is quite flat in magnitude over much of the outer area of the tube cross section. Table I gives Y_T^2 as a function of I at the radius of the maximum field. Using these numbers we may calculate $XY_T^2/2(1-X)^2$ and so infer from (3) and published "splittings" the required X (~ electron density) to support the plasma birefringence hypothesis. These calculations are presented in Fig. 3, and published splittings are summarized in Table II. Mode polarization and internal wavelength as a function of current measurements are now underway in this laboratory.

One series of polarization experiments has been published.[5] These experiments clearly show orthogonal polarization of the radiation for cavity length settings to either side of the peak power setting. Several further observations support the model. First, a spectral splitting does not appear under cw conditions where the magnetic field of the discharge current is a factor of 10^5 smaller. There is some ambiguity whether under pulsed operation the apparent doublet is observed when an external spectrometer is used to attempt to resolve it.[6,7] Second, time resolution of the current and laser pulses show that there is very little overlap for current pulses less than 180 A; the double mode has been reported only

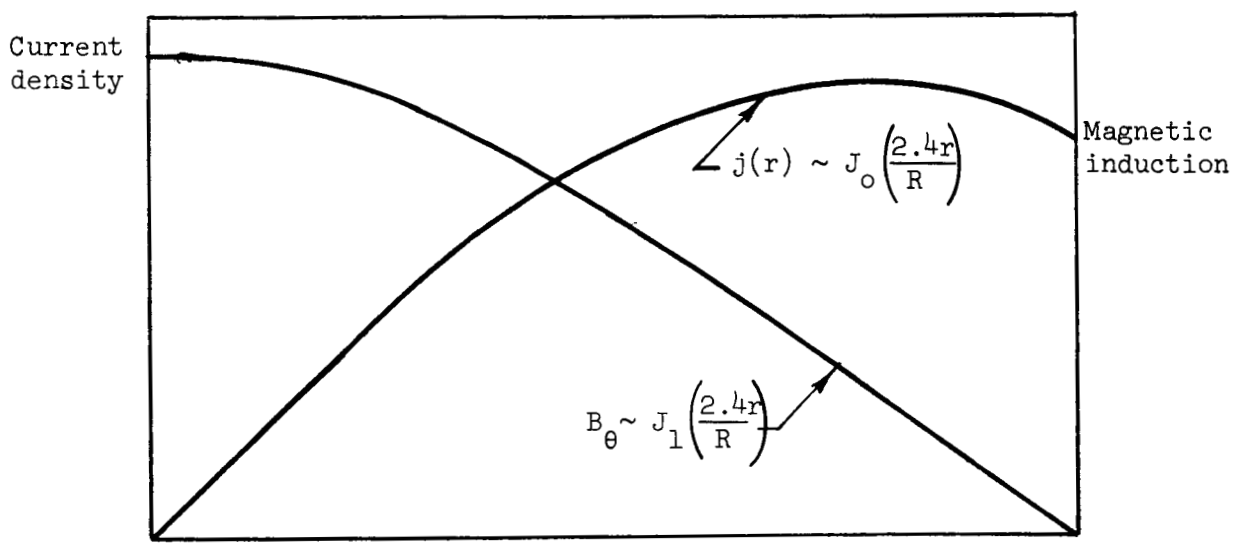

FIG. 2--Model for radial current density and magnetic induction distribution (arbitrary scales).

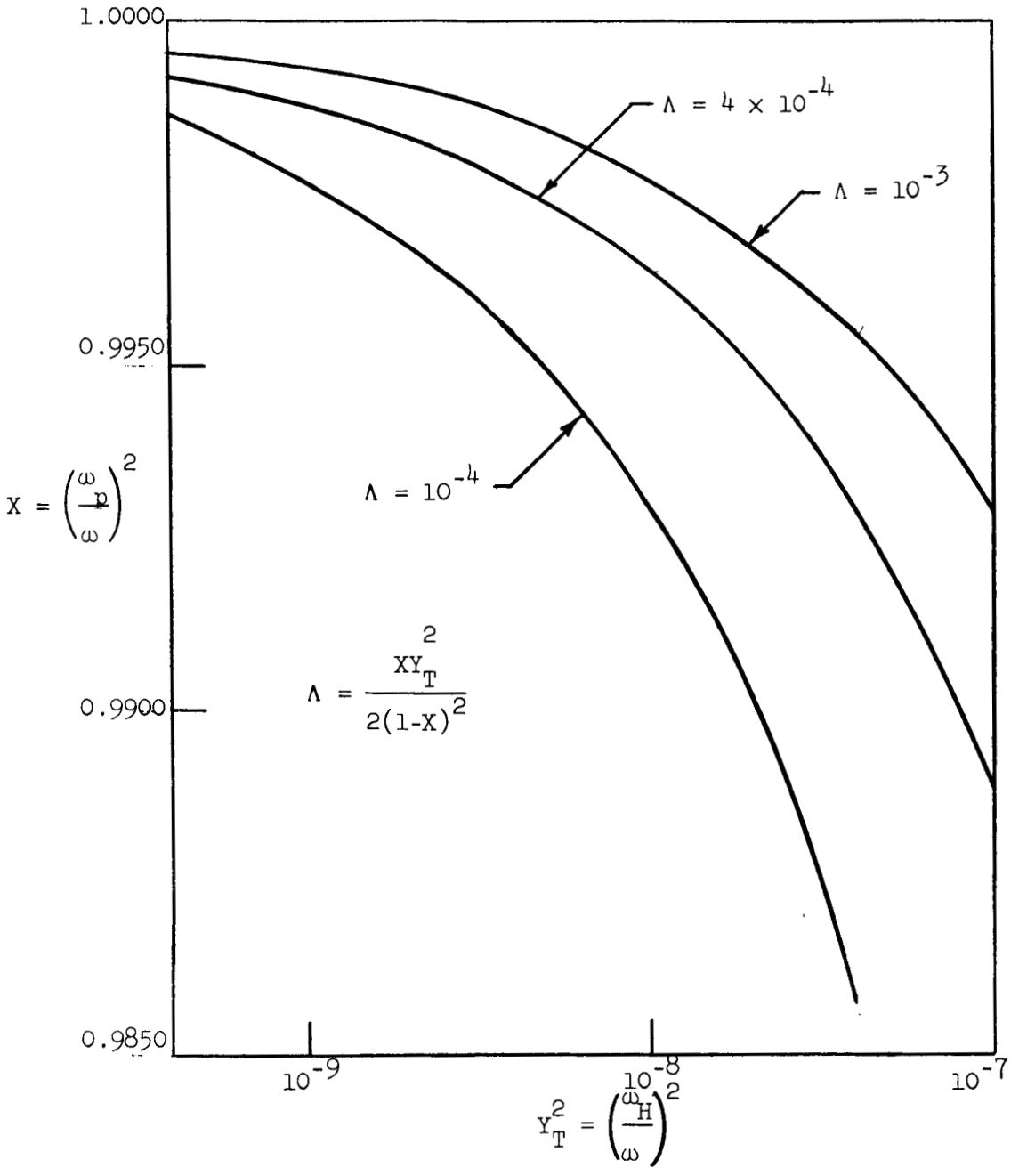

FIG. 3--Change in ratio of apparent wavelengths as a function of electron density and discharge current.

I	Y_T^2		$B_{\theta\ max}$
	337 μ	537 μ	
200 A	1.4×10^{-9}	2.0×10^{-9}	12 gauss
400	$5. \times 10^{-9}$	1.1×10^{-8}	24
600	1.2×10^{-8}	2.7×10^{-8}	36
1000	3.5×10^{-8}	9.0×10^{-8}	60

Table I. Calculated Y_T^2 at $B_{\theta\ max}$ for a simple electron density radial distribution and R = 3.7 cm.

Splitting (parts in 104)	Wavelength (μm)	Peak Current (or other data)	Reference
No	337	(17 kV)	10
Yes	337	(42 kV)	10
0.6	337	(52 kV)	10
2.8	337	(70 kV)	10
3	337	450 A	11
9	537	(~ 200 A)	11
Yes	337, others		12
1.5	337		7

Table II. Summary of published data where "splittings" were inferred from cavity tuning data.

for high current (e.g., 450 A for 337 μ), short-current-pulse (e.g., 1.5 μsec) conditions. Third, the implied electron density is generally consistent with the time delay between onset of current and laser pulses. The rate of electron density decay may be estimated using a volume electron-ion recombination model and extrapolating Stark broadening data for a hydrogen discharge having plasma parameters similar to those of the HCN laser.[9] This rate implies that without current flowing 0.2 μsec are required for X to fall from 1 to 0.997; for birefringence the laser pulse must occur during the current pulse, which lasts typically two microseconds.

Thus far we have neglected the role of electron collisions with ions, radical, atoms, and molecules. The average collision rate ν is introduced through a retarding force $m\nu\vec{v}$ in the electron equation of motion, where $\vec{v}$ is the electron velocity and where the average collision frequency is assumed to be the same for all electrons in the electron temperature distribution. This force has the effect of removing poles and zeros from the real and imaginary parts of the index of refraction. This force together with the electron density implied by the plasma birefringence hypothesis permit calculation of the light attenuation by the electrons provided one obtains a meaningful value for the average collision frequency. The collision frequency depends in turn on the imperfectly known electron temperature.

Assuming $X = 0.997$ implies a firm value for the ion density; applying the usual formula for electron and ion collision frequency in a partially ionized gas,[16] one obtains $Z = \nu/\omega = 10^{-2}$ and 10^{-3} for electron temperatures of 25,000° and 115,000°. The ordinary wave intensity

attenuation in dB/m equals 434 α where $\alpha/2 = (\omega/c)\mathrm{Im}(n)/\mathrm{cm}$ and $n^2 = 1\text{-}X/(1\text{-}iZ)$. The implied attenuations are of the order of 9800 and 1460 dB/m for $Z = 10^{-2}$ and 10^{-3}, respectively.

The laser gain required to overcome these extreme losses is conceivable for long-wavelength lasers. If the plasma berefringence hypothesis is proved correct by mode polarization and discharge current versus cavity length measurements, then the attractiveness of chemically pumped HCN lasers and amplifiers will be apparent. Power enhancement or stimulated emission on low-gain transitions could also be achieved using within the cavity a thin plasma mirror (a plasma Q-switch) which would permit the electron density of the pumping discharge to decrease over a fraction of the lifetime of the inverted state. For instance, a 10 μsec delay reduces X from 0.997 to 0.87 on the volume electron-ion recombination model, and the attenuation for $Z = 10^{-2}$ and 10^{-3} is reduced to 2140 and 192 dB/m, respectively.

The implied attenuation requires that mode analysis include the radial and axial variation of refractive index and attenuation, which is not carried out here. It is clear from experimental data that off-axis modes are favored.[13]

It is necessary to comment on the approximation in (5), which is essentially that $Y_T \ll 1\text{-}X$ at the moment of laser pulse onset. Should this condition not be met and certain other conditions obtain, a temporal fine structure is predicted to appear. The extraordinary mode appears first, then the ordinary mode, followed by the possible disappearance and reappearance of the extraordinary mode, according to $n = 0$ for $X = 1$ while $n_x = 0$ for $X = 1\text{-}Y$. This phenomenon would be similar to the triple splitting of radio propagation studies.[14]

Longitudinal Magnetic Field

We now investigate the plasma effects for continuous-wave far infrared lasers for the case of applied longitudinal magnetic fields. Here the electron density is perhaps a factor of 10^4 less than the plasma resonace density, and the magnetic effects of the discharge current are negligible. For $\theta = 0$, $Y_T = 0$ one obtains from (1) and (2) two modes, r and l , right- and left-circularly polarized:

$$n_{r\,\ell}^2 = 1 - \frac{X}{1 \pm Y_L} \qquad , \quad \rho = \mp i$$

$$\frac{n_r}{n_\ell} = \sqrt{\frac{1 - X - Y_L^2 + XY_L}{1 - X - Y_L^2 - XY_L}} = 1 + \frac{L_\ell - L_r}{L_r} \qquad (6)$$

Substitution of plausible number reveals that these effects are potentially observable. These effects may well be involved in the HCN laser observations of footnote 5 of reference 3.

Applying the plasma birefringence hypothesis to the data of reference 15 one obtains a close match to the proposed "$g_e = 0.78$" Zeeman splitting curve of Fig. 2b of this reference by assuming (6) and an electron density of $3.2 \times 10^{13}/cm^3$. (The implied intensity attenuation due to electrons is about 2 and 0.2 dB/m for $Z = 10^{-2}$ and 10^{-3} , respectively, and it is negligibly different for the two modes.) It appears necessary in this case to measure the electron density and temperature, calculate the birefringence and attribute residual splittings to molecular magnetic effects.

In summary, the study during the report period of the effects of electron density on laser behavior has yielded very interesting predictions. It is hoped during the next period that through measurement of polarization as a function of current and laser pulse overlap the birefringence hypothesis can be confirmed or denied. If the hypothesis is confirmed, efforts will be made to increase power output through Q-switching or chemical inversion; if denied the longitudinal magnetic field plasma effects will be demonstrated.

REFERENCES

1. See, for example, K. G. Budden, Radio Waves in the Ionosphere (Cambridge University Press, 1961).
2. Suggested by E. Brannen, V. Sochor, W. J. Sarjeant, and H. R. Froelich, Proc. IEEE 55, 462 (1967).
3. L. O. Hocker, A. Javan, D. R. Rao, L. Frenkel, and T. Sullivan, Appl. Phys. Letters 10, 147 (1967).
4. See, for example, C. G. B. Garrett, Gas Lasers (McGraw-Hill, 1967), p. 50.
5. A. Hadni, R. Thomas, and J. Weber, Journal de Chimie Physique 64, 71 (1967).
6. P. Schwaller, H. Steffen, J. F. Moser, and F. K. Kneubühl, Appl. Optics 6, 827 (1967).
7. H. Steffen, J. F. Moser, and F. R. Kneubühl, J. Appl. Phys. 38, 3410 (1967).
8. V. Sochor and E. Brannen, Appl. Phys. Letters 10, 232 (1967).
9. J. M. Wilcox, A. W. DeSilva, W. S. Cooper III, and F. I. Boley, Radiation and Waves in Plasmas, M. Mitchner, ed., (Stanford University Press, 1961), p. 138.
10. M. Camani, F. K. Kneubühl, J. F. Moser, and H. Steffan, Z. angew. Math. Phys. 16, 562 (1965).

11. H. Steffan, P. Schwaller, J. F. Moser, and F. K. Kneubühl, Phys. Letters 23, 313 (1965).

12. W. Prettl and L. Genzel, Phys. Letters 23, 443 (1966).

13. S. Kon, M. Yamanaka, J. Yamamoto, and H. Yoshinaga, Jap. J.Appl.Phys. 6, 612 (1967).

14. J. A. Ratcliffe, The Magneto-Ionic Theory,(Cambridge University Press, 1959), p. 126.

15. W. J. Tomlinson, M. A. Pollack, and R. L. Fork, "Zeeman Effect Studies of the Water-Vapor Laser Oscillating on the 118.65 μm Transition," Appl. Phys. 11, 150 (1967).

16. G. Bekefi, Radiation Processes in Plasmas (John Wiley, 1966), p. 99.